YILDIZ TECHNICAL UNIVERSITY
DEPARTMENT OF MECHANICAL ENGINEERING

MATHEMATICAL MODELLING AND NUMERICAL SIMULATION OF SPRAY DRYING PROCESS

22065608 SEFA ÇİÇEK

PROJECT 1

Advisor: Professor Dr, Hakan, Demir

İSTANBUL, 2025

CONTENTS

LIST OF ICONS

c	Specific heat
h	Enthalpy
T	Temperature
P	Pressure
W	Moisture content
X	Moisture content
H	Enthalpy
Q	Mass flow rate
m	Mass
k	Thermal conductivity
h_c	Convection heat transfer coefficient
D_{diff}	Diffusion coefficient
k_g	Mass transfer coefficient
v	Velocity
Re	Reynolds number
Pr	Prandtl number
Sc	Schmidt number
Nu	Nusselt number
Sh	Sherwood number
C_D	Drag coefficient
A	Surface area
V	Volume

Greek Letters

ω	Absolute humidity
ϕ	Relative humidity
μ	Viscocity
ρ	Density
π	Pi number

Indices

a	Air
p	Particle
pL	Liquid Particle
s	Solid feed

Bases

. (dot)	unit time

LIST OF ABBREVIATIONS

CFD	Computational Fluid Dynamics
ASME	American Society of Mechanical Engineers
DPM	Discrete Phase Model

LIST OF FIGURES

LIST OF TABLES

ABSTRACT

In this study, the spray drying process is analyzed both theoretically and numerically. The primary objective of the project is to model and simulate the heat and mass transfer phenomena that occur during the drying of liquid products such as milk, which are atomized into fine droplets and exposed to hot air for rapid moisture removal. The study is carried out in two main stages: the development of a theoretical model using MATLAB and a numerical simulation using ANSYS Fluent.

In the theoretical phase, a one-dimensional axial plug-flow model was developed under the assumption of co-current flow between air and droplets. The model was implemented in MATLAB to predict how droplet properties — such as temperature, diameter, and moisture content — evolve along the drying chamber. The governing equations are based on energy and mass conservation laws, and the transfer coefficients are determined using empirical correlations available in the literature. Convective heat transfer and evaporative mass transfer are considered as the dominant mechanisms between the drying air and the droplets. The model accounts for variations in air temperature, velocity, and humidity along the axial direction of the chamber.

The second stage of the study involves numerical simulation using ANSYS Fluent, aiming to validate the theoretical model and gain deeper insight into the fluid-dynamic and thermodynamic behavior of the drying system under more realistic conditions. A CFD (Computational Fluid Dynamics) approach is used, with the air phase modeled as continuous (Eulerian) and the droplet phase as discrete (Lagrangian). The evaporation of droplets is simulated using the Discrete Phase Model (DPM), which enables the tracking of individual droplet trajectories and their interactions with the air phase. Two-way coupling is employed to consider momentum and energy exchanges between the phases. The boundary conditions, droplet injection parameters, and air inlet properties are defined to match the theoretical setup as closely as possible.

Results from both the MATLAB model and ANSYS Fluent simulations show consistent trends, particularly in droplet temperature drop, moisture loss, and shrinkage along the flow direction. The comparison between theoretical and numerical outcomes indicates that the simplified model can provide reasonably accurate predictions, which is valuable for quick parametric studies and preliminary design evaluations. On the other hand, the CFD model offers more detailed spatial information and reveals complex interactions such as turbulence, recirculation zones, and localized drying rates.

Overall, this study contributes to the understanding of spray drying processes by providing a comprehensive analysis that combines theoretical modeling and advanced numerical simulation. The results can support the design, optimization, and scale-up of industrial spray dryers, especially for food and pharmaceutical applications where product quality and energy efficiency are critical concerns.

Key Words: Spray Drying, CFD, DPM

1. INTRODUCTION

Spray drying is one of the most widely utilized techniques for converting liquid materials into dry powders, particularly in the food, pharmaceutical, and chemical industries. Its ability to produce fine, uniform, and stable particles with controlled moisture content makes it an indispensable process for preserving thermally sensitive products, improving shelf life, and facilitating easier handling and transport. Among various applications, spray drying plays a vital role in dairy product manufacturing, such as in the production of milk powder, due to its efficiency, scalability, and ability to retain nutritional quality.

Given the growing global demand for powdered food products and pharmaceuticals, optimizing spray drying systems has become increasingly important. However, the process is inherently complex, involving simultaneous heat and mass transfer between the hot drying air and atomized liquid droplets, which undergo rapid evaporation, temperature change, and sometimes structural transformations. These phenomena are highly dependent on operating parameters such as inlet air temperature, droplet size distribution, air velocity, and chamber geometry. As a result, both experimental and computational studies have been extensively carried out to understand and improve spray drying performance.

In recent years, advances in numerical methods, particularly Computational Fluid Dynamics (CFD), have provided powerful tools for simulating spray drying processes in detail. CFD allows for the prediction of temperature fields, velocity profiles, humidity distribution, and droplet behavior within the drying chamber, offering insights that are difficult to obtain experimentally. Meanwhile, simplified theoretical models based on mass and energy balance equations are still widely used for quick parametric analysis and initial design estimations. These models, when validated against experimental or numerical data, provide a reliable basis for process understanding and optimization.

Despite the progress in modeling and simulation, achieving an optimal balance between product quality, energy consumption, and process efficiency remains a challenge. Many industrial spray dryers still operate based on empirical adjustments, which can lead to inconsistent product quality and unnecessary energy losses. Therefore, there is a growing need for systematic studies that integrate theoretical modeling with detailed numerical simulations to better understand the physics of spray drying and to aid in the

rational design of equipment and processes.

This project aims to contribute to this ongoing effort by developing a one-dimensional theoretical model of the spray drying process using MATLAB and validating the model through numerical simulations carried out in ANSYS Fluent. The focus is on analyzing the heat and mass transfer mechanisms governing the drying of milk droplets under co-current flow conditions. By comparing theoretical and CFD results, this study seeks to evaluate the accuracy of simplified models and explore the potential of CFD as a design and optimization tool. The findings are expected to assist in improving the design of spray drying systems, particularly in applications where thermal efficiency and product quality are of paramount importance.

2. LITARATURE REVIEW

Spray drying has been a topic of extensive research due to its widespread use in various industries, particularly in the production of food powders, pharmaceuticals, and chemicals. Over the past several decades, numerous experimental and computational studies have been conducted to better understand the complex mechanisms of droplet drying, heat and mass transfer, and the resulting product characteristics. The literature reveals a significant evolution in both the modeling techniques and simulation tools applied to the spray drying process.

Early studies on spray drying primarily focused on experimental investigations to understand the relationship between process parameters and product quality. Researchers such as Masters (1991) and Filkova & Mujumdar (1995) provided foundational knowledge on spray dryer design, droplet formation, and drying kinetics. These studies emphasized the critical role of parameters such as inlet air temperature, droplet size, and residence time in determining the final moisture content and particle morphology. However, experimental methods were often limited by the difficulty of measuring droplet-level behavior inside industrial-scale dryers.

To overcome these limitations, simplified mathematical models were introduced, particularly plug-flow and well-mixed models, to describe the behavior of droplets as they travel through the drying chamber. One-dimensional axial models became popular for their ability to predict droplet temperature, moisture content, and shrinkage along the chamber's length. These models often assume spherical droplets, uniform flow, and steady-state conditions. An example of such a model is the one presented by Langrish and Zbicinski (1994), which has been widely referenced and expanded upon in later works.

With the advancement of computing power and numerical techniques, Computational Fluid Dynamics (CFD) has become an essential tool in spray drying research. CFD models typically employ an Eulerian-Lagrangian approach, where the air is treated as a continuous phase and the droplets as discrete particles. The Discrete Phase Model (DPM), often used within ANSYS Fluent and similar solvers, allows the simulation of droplet trajectories, evaporation, and interactions with the surrounding air. Studies by Huang et al. (2006), Kiranoudis et al. (1999), and more recently by Mezhericher et al. (2008) have demonstrated the ability of CFD to predict complex flow patterns,

temperature fields, and drying efficiency in spray dryers.

Recent literature has also highlighted the importance of coupling heat and mass transfer with particle shrinkage, crust formation, and internal diffusion within droplets. Advanced models now consider multicomponent evaporation, variable thermal properties, and transient effects to improve the accuracy of predictions. Some works even integrate CFD with population balance models (PBM) to capture the evolution of droplet size distributions during drying.

Despite significant progress, challenges remain in achieving a balance between model complexity and computational cost. As a result, researchers continue to explore hybrid approaches, where simplified theoretical models are validated and refined using detailed CFD simulations. This dual approach allows for rapid evaluation of design parameters while maintaining high-fidelity predictions of dryer performance.

In conclusion, the literature clearly demonstrates that integrating theoretical modeling with CFD simulation offers a robust framework for analyzing spray drying processes. These methods are critical for optimizing dryer design, enhancing energy efficiency, and ensuring consistent product quality in modern spray drying applications.

3. DESCRIPTION OF PROBLEM

3.1 Spray Drying Fundementals

Spray drying is typically divided into four fundamental stages:

- Atomization of feed into spray,
- Spray-air contact
- Drying of spray (drying phase),
- Separation of the dried particles from the air stream.

Each stage is governed by the specific design and operational parameters of the spray dryer. In combination with the physicochemical properties of the feed material, these factors collectively influence the characteristics of the final dried product.

Figure 3.1 schematically illustrates the functional elements associated with each processing stage.

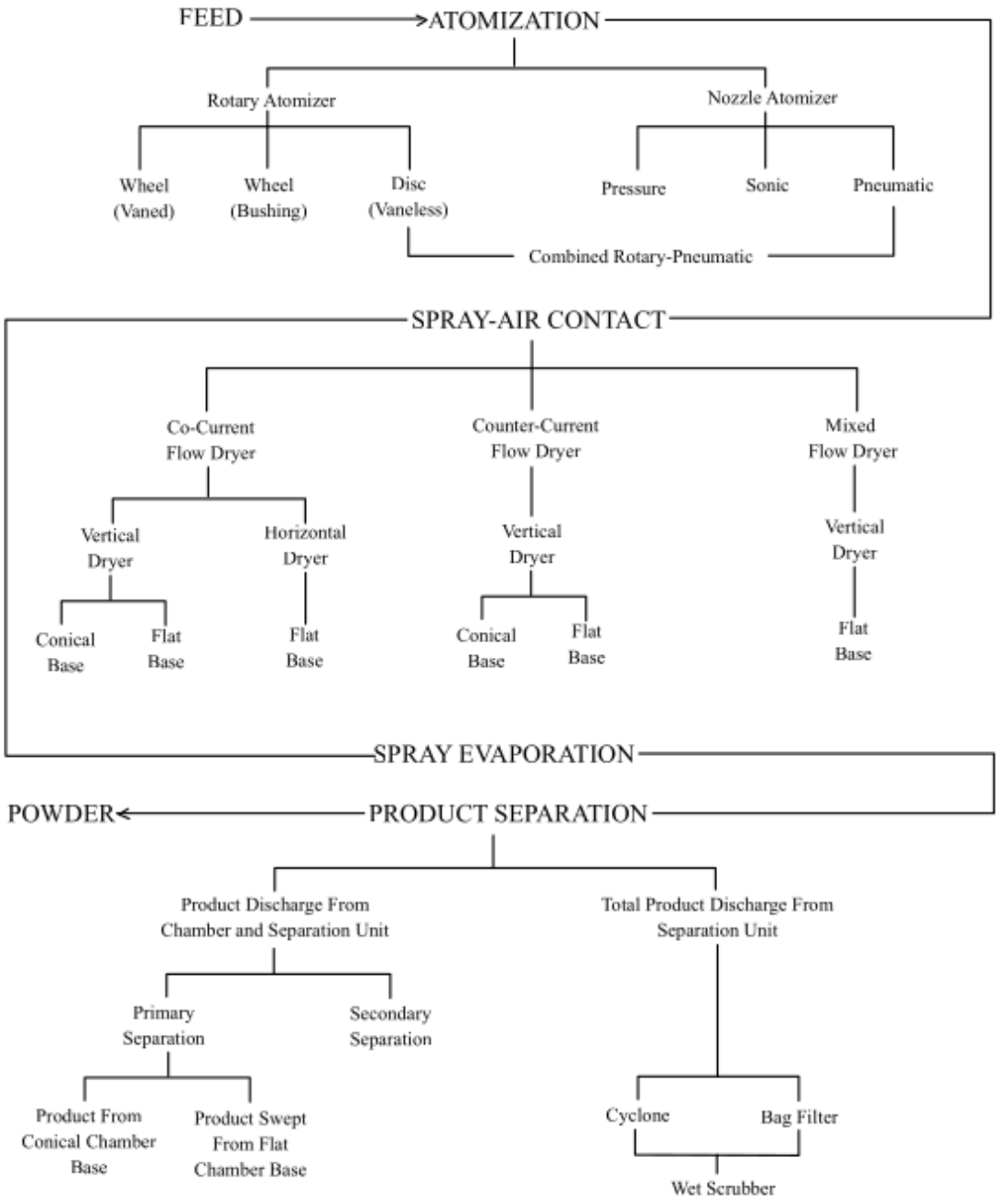

Figure 3.1. Schematic of spray drying process shown in stages. [13]

Figure 3.2 presents the standard equipment configuration required to implement these stages, including a atomizer, cyclone separators, and a conveying system.

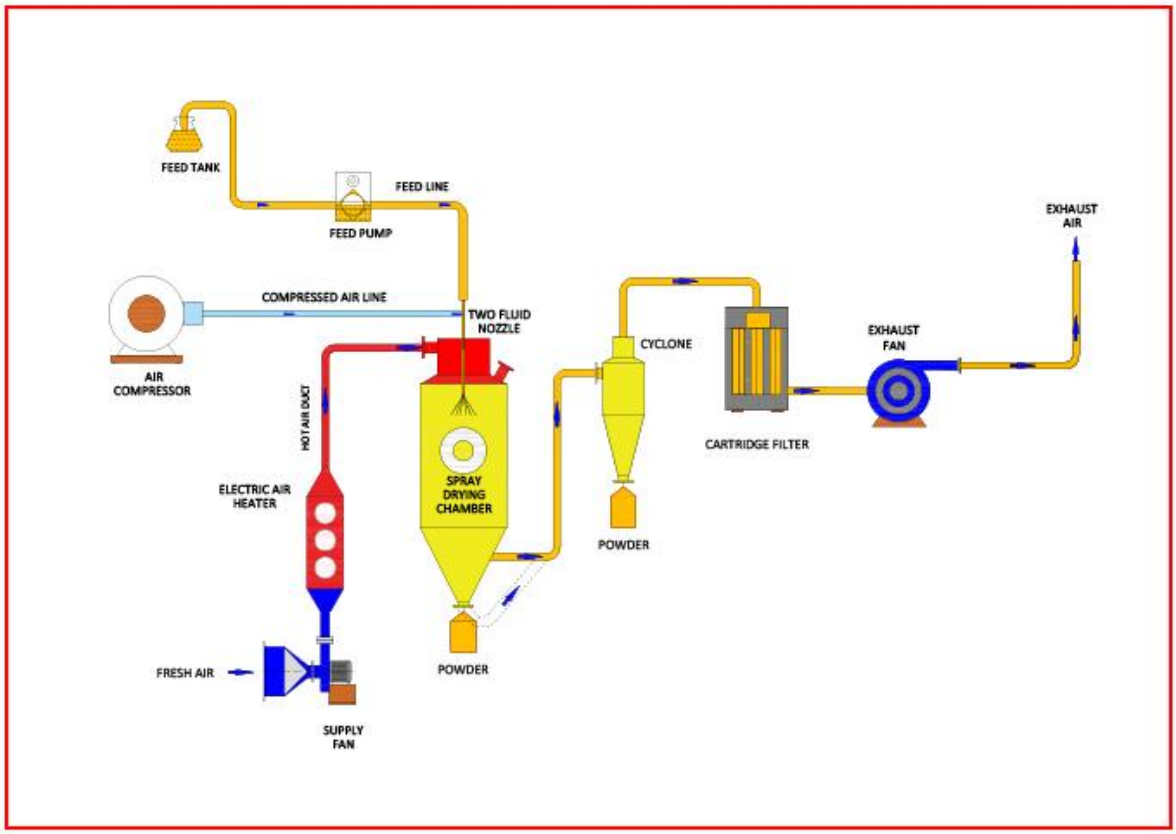

Figure 3.2. Equipment involved in a standard spray dryer layout. [20]

In this setup, feed is pumped from the product feed tank to a atomizer, which is located at the top of the drying chamber. Drying air is drawn from the ambient environment using a supply fan, then heated via steam before being introduced into the chamber. As the atomized spray encounters the heated air, rapid drying occurs within the chamber. The majority of the dried particles descend to the chamber base and are discharged through a powder outlet into a pneumatic conveying system. The conveying air is pre-filtered to prevent contamination. Finer particles that remain suspended in the air stream are transported to cyclone separators, where they are removed from the air and also conveyed pneumatically. The cleaned exhaust air is finally released into the atmosphere via an exhaust fan. The dried powder conveyed pneumatically is collected at the bottom of the transport cyclone. The system is equipped with various instrumentation components, including air temperature sensors positioned at strategic locations, a pressure gauge for monitoring the drying chamber pressure, and adjustable dampers to regulate airflow throughout the process.

3.1.1 Atomization of Feed into a Spray

Atomization and the subsequent interaction of the spray with drying air are the defining operations in spray drying processes. The performance and operational characteristics of the atomizer play a critical role in ensuring cost-effective production while maintaining high product quality. Effective atomization must produce a spray that facilitates optimal evaporation conditions, ultimately resulting in a dried product with the desired physical and functional attributes.

Sprays in industrial systems are typically generated using rotary atomizers or nozzles. Rotary atomizers employ centrifugal force and are generally categorized into two types: Atomizer wheels, and Atomizer discs. Wheel-based atomizers are capable of processing feed rates in the range of several tens of tons per hour. In contrast, nozzle atomization relies on pressure-driven, kinetic, or in some cases, sonic energy to produce sprays. A broad array of nozzle types and sizes exists to accommodate diverse spray drying requirements. However, individual nozzle units generally have lower feed capacity compared to rotary atomizers, often necessitating the use of multiple nozzles in parallel when processing high feed volumes.

The choice of atomizer is determined by the characteristics of the feed material (e.g., viscosity, surface tension, thermal sensitivity) and the desired properties of the final dried product (e.g., particle size, morphology). Regardless of the atomizer type, increased energy input during atomization typically yields smaller droplet sizes, which enhances evaporation efficiency. Conversely, if the atomization energy remains constant but the feed rate increases, the resulting spray will consist of larger droplets. Additionally, fluid properties significantly affect atomization: feeds with higher viscosity or surface tension will produce larger droplets under the same energy input due to their greater resistance to deformation.

Figure 3.3. Atomizers in operation [19]

3.1.2 Spray-Air Contact

The mode of interaction between the spray and the drying air is a critical parameter in spray dryer design, as it significantly affects the behaviour of droplets during drying and consequently influences the characteristics of the final dried product. the pattern of interaction between the spray and the drying air is primarily determined by the position of the atomizer relative to the drying air inlet. Various configurations are possible; for instance, the spray may be directed into the stream of hot air entering the drying chamber, as illustrated in Figure 3.3(a). In this configuration commonly referred to as 'co-current flow' due to the parallel direction of air, feed, and product flow—both the drying air and the atomized liquid move in the same direction through the chamber.

This arrangement is widely employed, particularly for drying heat-sensitive materials, due to its ability to minimize thermal degradation. Evaporation occurs rapidly as the hot air contacts the droplets, leading to a rapid decrease in air temperature and a corresponding reduction in evaporation time. During the majority of the drying process, the temperature of the droplets remains close to the wet bulb temperature, thereby keeping the product temperature low and protecting it from heat damage. As the product approaches its target moisture content, its temperature remains relatively low since it is exposed to significantly cooler air.

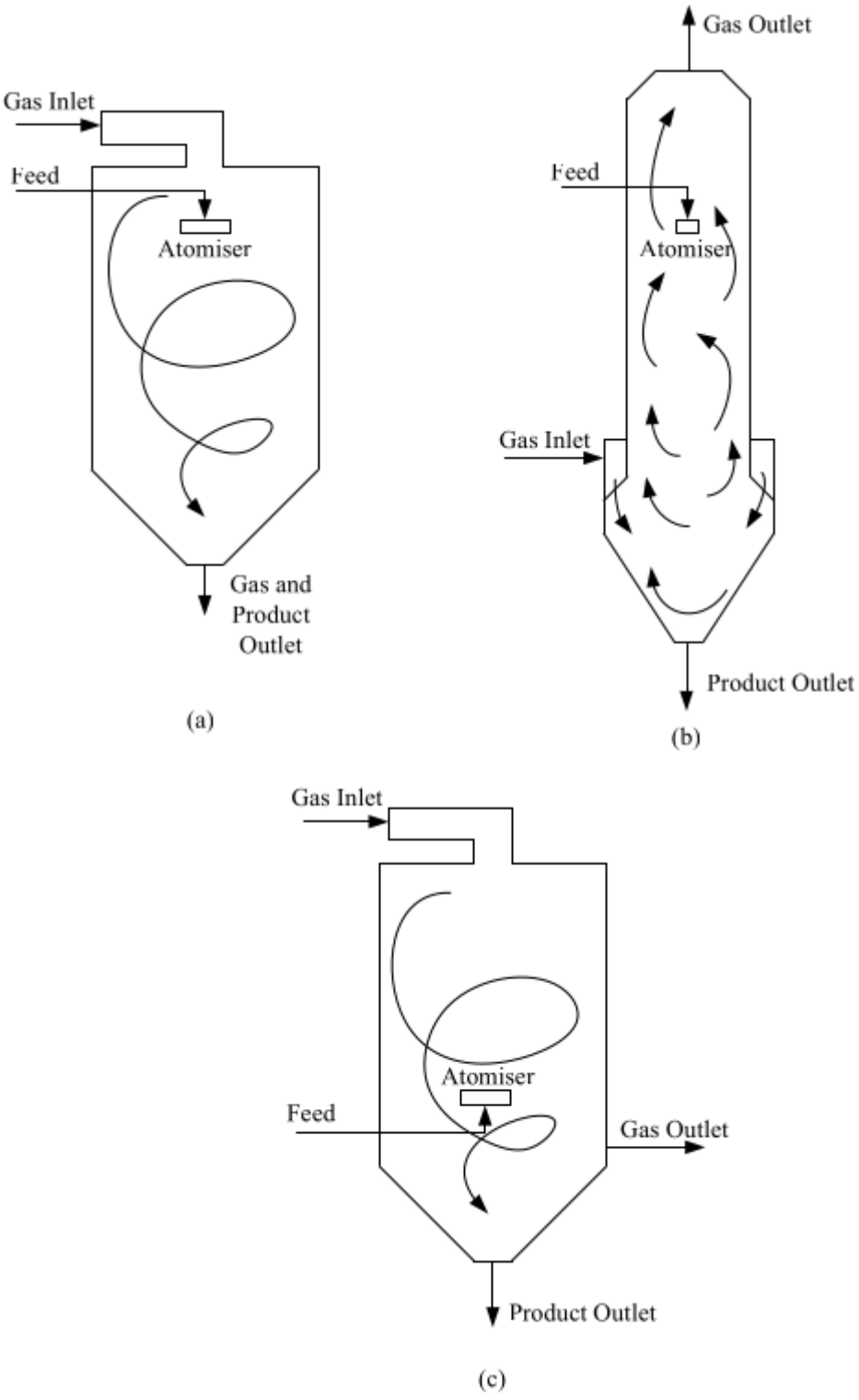

Figure 3.4. Spray-Air Contact: (a) Co-current flow; (b) Counter-current flow; (c) Mixed flow [13]

Alternatively, the spray may come into contact with the drying air in a 'counter-current' flow configuration, as illustrated in Figure 3.4(b), wherein the spray and the air enter the drying chamber from opposite ends. This configuration is characterized by efficient thermal energy utilization; however, it exposes the already dried powder to the hottest incoming air stream. Despite this drawback, counter-current flow is particularly suitable for the production of granular powders from non-heat-sensitive materials. It is frequently employed in conjunction with nozzle atomizers. In such systems, the upward flow of drying air opposes the downward motion of larger droplets, effectively reducing their terminal velocity. This allows for prolonged residence time within the drying chamber, thereby ensuring complete evaporation prior to particle discharge.

Mixed flow dryers, which combine both co-current and counter-current flow configurations as shown in Figure 3.4(c), allow for the production of coarse, free-flowing powders within relatively compact drying chambers.

In all cases, the airflow pattern plays a key role in determining the rate and extent of evaporation. It affects how the spray moves through the drying zone, influences the concentration of particles near the dryer walls, and controls how much of the partially dried droplets return to the hot regions around the air disperser.

3.1.3 Drying of Spray

When spray droplets come into contact with the drying air, evaporation begins immediately from a saturated vapor layer that quickly forms on the droplet surface. The surface temperature of the droplet closely matches the wet bulb temperature of the drying air. Evaporation occurs in two distinct stages.

In the first stage, known as the constant rate period, the droplet contains enough internal moisture to replace the water evaporating at the surface. Moisture continues to diffuse from the interior to the surface, maintaining saturation conditions. During this phase, the evaporation rate remains steady.

As drying continues and the moisture content decreases to a level where saturation at the surface can no longer be maintained, the critical moisture point is reached. At this stage, a dried shell begins to form on the droplet surface. From this point on, evaporation becomes limited by the rate at which moisture can diffuse through this dried layer. This second stage is called the falling rate period, during which the

evaporation rate gradually declines as the shell thickens over time.

Because much of the evaporation occurs while the droplet surface remains saturated and cool, the product temperature stays low. The design of the drying chamber and the airflow rate are adjusted to ensure that the droplets remain in the chamber long enough for the desired moisture removal to occur, but are discharged before their temperature can approach that of the hot outlet air. This minimizes the risk of thermal damage to the product.

3.1.4 Separation of Dried Product from the Air

After the drying process is completed and the dried particles remain suspended in the air, product separation from the drying air takes place. Two common recovery systems are used for this purpose. Figure 3.5 illustrates these systems for co-current flow dryers equipped with a rotary atomizer and cyclone separators.

System (1): In this system, primary separation of the dried product occurs at the bottom of the drying chamber (Figure 3.5(a)). Most of the dried material settles at the chamber base during operation, while a smaller portion remains airborne and exits with the drying air. This airborne fraction is then recovered using separation equipment such as cyclones, which are most commonly used. In some cases, bag filters, electrostatic precipitators, or wet scrubbers may also be employed, depending on the concentration of powder in the exhaust air and the required recovery efficiency.

This system also results in a natural classification of the powder: coarse particles are collected at the base of the chamber, while finer particles are recovered by the separation equipment. Although this particle size separation can be beneficial, in standard practice, both fractions are usually recombined and transported to a single discharge point.

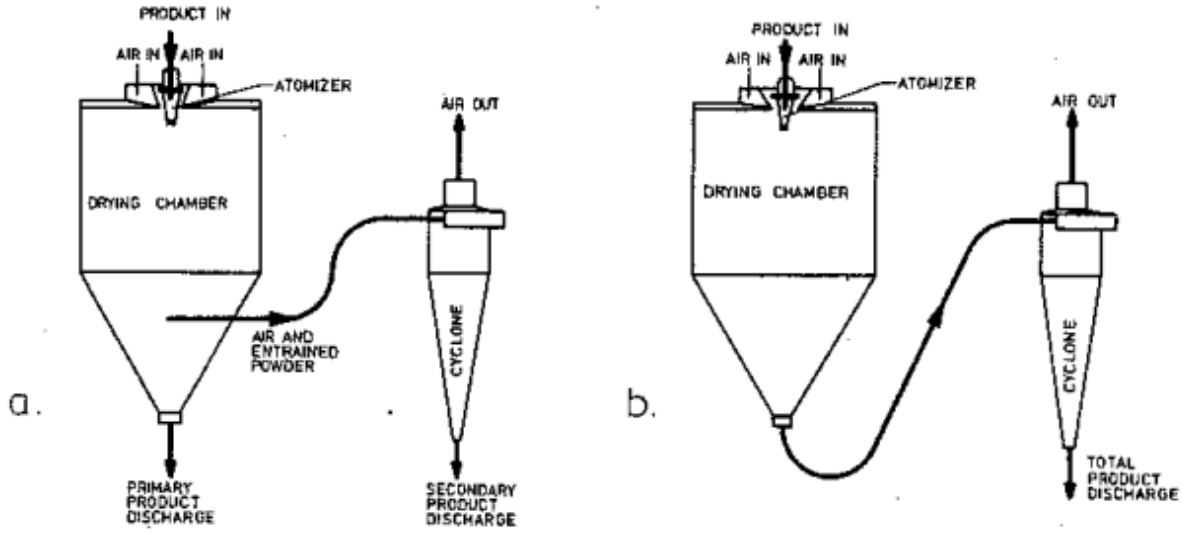

Figure 3.5. Product discharge from co-current flow spray dryers.[1]

System (2): In this system, the entire recovery of the dried product occurs within the separation equipment (Figure 3.5(b)). As a result, the efficiency of the separation device becomes critically important. Despite this requirement, the system is frequently used because it eliminates the need for an additional product conveying mechanism from the drying chamber, simplifying the overall process layout.

3.2 Drying Terms and Principles

Drying is defined as the removal of water from a material to the extent that the remaining solids are in a completely or nearly moisture-free state. In a feed material, moisture exists in two main forms: bound moisture and unbound moisture. The drying behavior of a substance depends on the characteristics of both the solid and the moisture it contains. Bound moisture refers to water that is held within the solid in such a way that it exerts a vapor pressure lower than that of pure water at the same temperature. This type of moisture may be trapped in fine capillaries, adsorbed on solid surfaces, dissolved in the structure of cells or fibers, or chemically bound (such as water of crystallization). Unbound moisture, in contrast, is the water present in excess of the

bound moisture in a hygroscopic material. In non-hygroscopic materials, all the moisture is considered unbound and behaves like pure water, exerting a vapor pressure equal to that of pure water at the same temperature. The equilibrium moisture content is the amount of moisture a material retains when it is in balance with the water vapor pressure in its surrounding environment. The free moisture is the amount of water that exceeds this equilibrium value. Free moisture includes unbound water and, in some cases, a portion of the bound water. Importantly, only free moisture can be removed through evaporation during the drying process.

During spray drying, moisture moves within the droplet primarily through diffusion, with capillary flow also contributing to the process. The drying behavior of a droplet depends on whether bound or unbound moisture is being removed, as each type influences drying differently. As long as unbound moisture is present, the drying occurs at a constant rate, provided that the internal moisture transport (via diffusion and capillary action) is fast enough to keep the droplet surface saturated. Drying at this stage is efficient and steady. When the rate of internal moisture movement becomes insufficient to maintain saturated conditions at the surface, the critical point is reached. Beyond this point, the drying rate begins to decrease. This marks the start of the falling rate period, which continues until the droplet reaches its equilibrium moisture content—the point at which the moisture level of the product matches the vapor pressure of its surrounding air. At this equilibrium, no further moisture removal occurs unless environmental conditions change.

Figure 3.6 illustrates how these concepts apply to the drying behavior of a spray droplet in an air medium with constant humidity. Additional commonly used terms related to drying mechanisms are summarized below the figure.

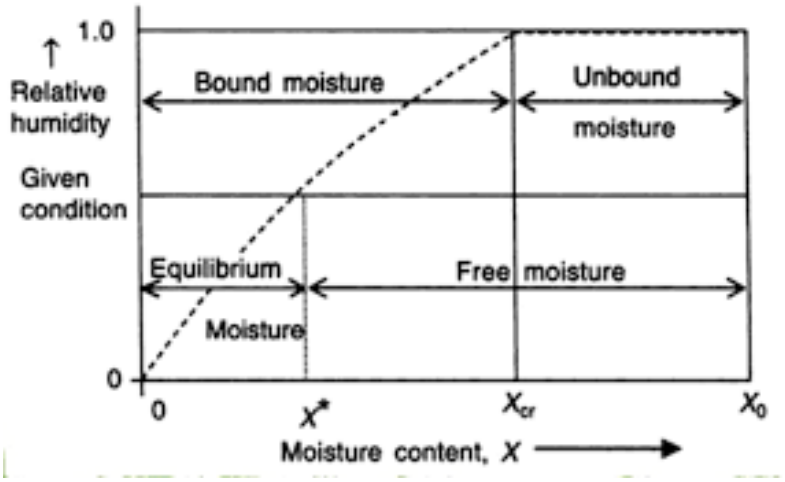

Figure 3.6. Graphical relation between common drying terms. [18]

Dry air refers to atmospheric air that does not contain water vapor, in contrast to wet air, which includes water vapor. The amount of water vapor in the air can vary significantly depending on location, weather, and time of day.

The properties of wet air are typically analyzed using psychrometric charts, which provide a graphical representation of the thermodynamic properties of moist air. These charts usually relate air temperature and humidity, or enthalpy and humidity, with the former being more commonly used.

In a standard psychrometric chart:

- The horizontal axis (abscissa) represents the dry bulb temperature (the temperature of air measured by a regular thermometer).
- The vertical axis (ordinate) shows the absolute humidity, which is the mass of water vapor per unit mass of dry air.
- Relative humidity is shown as a set of curved lines across the chart.
- Other properties such as air volume, total heat content (enthalpy), and wet bulb temperature are also displayed, providing a comprehensive view of moist air behavior under various conditions.

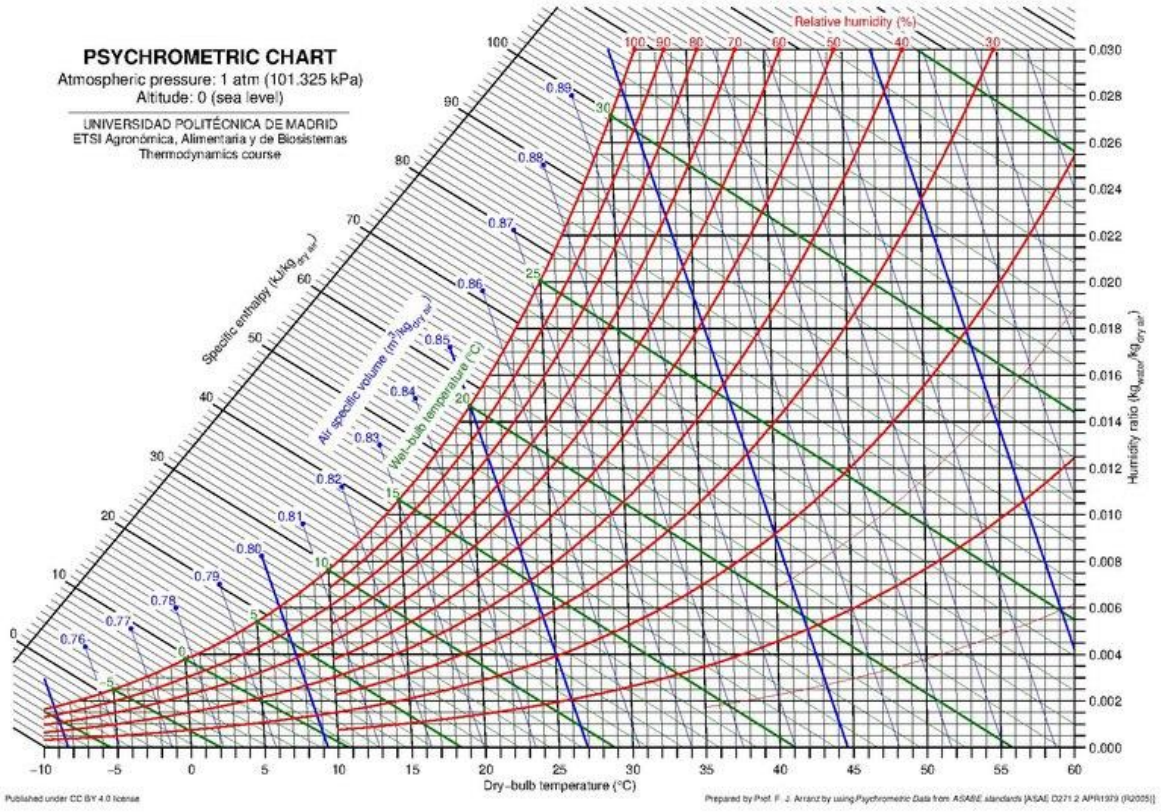

Figure 3.7. Physchrometric chart. [17]

Humidity refers to the amount of water vapour in the air. While the quantity of water vapour does not depend on the total air pressure (P), it is affected by the temperature of the air it is mixed with. This relationship is explained by Dalton's Law. Therefore, in air–water systems, the absolute humidity (ω) is associated with the partial pressure (P_W) of water vapour in the air as follows:

$$\omega = \frac{18}{29}\left(\frac{P_W}{P - P_W}\right) \tag{3.1}$$

Where ω is expressed as

$$\frac{weight\ of\ water\ vapour}{unit\ weight\ of\ dry\ air}\left(\frac{kg}{kg}\right)$$

Relative humidity (ϕ) refers to the amount of water vapour in the air compared to the maximum amount that the air can hold at the same temperature (i.e., saturation). When

the air is fully saturated, the relative humidity is defined as 100%. Alternatively, relative humidity can also be expressed as a ratio.

$$\phi = 100\left(\frac{partial\ pressure\ of\ water\ in\ air\ at\ temp\ (T)}{vapour\ pressure\ of\ water\ at\ temp\ (T)}\right) \tag{3.2}$$

Atmospheric air consists of dry air and water vapour. Therefore, the enthalpy of air is described by the enthalpies of both dry air and water vapour. In most practical cases, the amount of dry air in the air–water vapour mixture stays constant, while the amount of water vapour varies. For this reason, the enthalpy of atmospheric air is expressed per unit mass of dry air, rather than per unit mass of the entire air–water vapour mixture. The total enthalpy (an extensive property) of atmospheric air is the sum of the enthalpy of dry air and the enthalpy of water vapour:

$$h = h_a + \omega h_g \tag{3.3}$$

3.3 Heat and Mass Balances over Spray Dryers

Heat and mass balances are established based on Figure 3.8. For calculating the enthalpies of both the inlet air and the product, the reference temperature is taken as the freezing point of water. In moisture balance calculations, it is common to use a unit mass of bone-dry product as the basis. Assume that $\dot{m}_s$ (in weight units per hour) of dry solid enters the spray dryer as part of a feed (such as a solution, slurry, or paste) containing W_1 units of moisture per unit of dry solid. The drying process reduces the moisture content of the solid to W_2 units of moisture per unit of dry solid. The temperature of the feed at the moment of atomization is T_{s1}, while the product leaves the dryer at a temperature of T_{s2}. Drying air is introduced into the dryer at a rate of $\dot{m}_a$ (in weight units of dry air per hour) and at a temperature of T_{a1}. The inlet absolute air humidity is ω_1, and increases during the dryer operation to ω_2. The air leaving the dryer is T_{a2}.

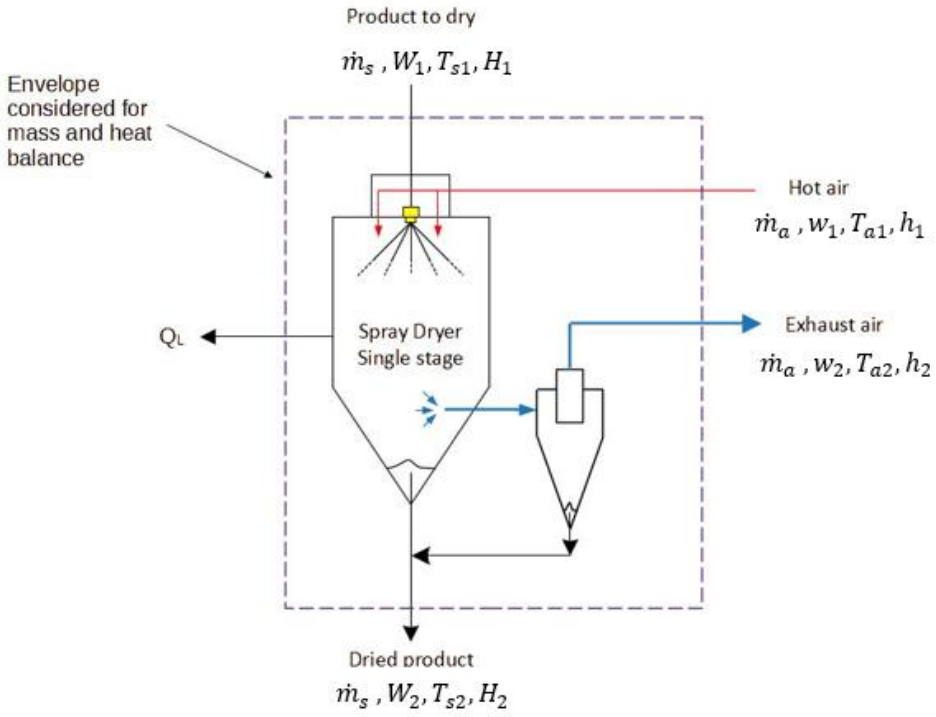

Figure 3.8. Dryer data for calculation of heat and mass balances.[2]

Mass balance

For no product accumulation in the chamber

$$input = output \tag{3.4}$$

thus:

$$\dot{m}_a\omega_1 + \dot{m}_s W_1 = \dot{m}_a\omega_2 + \dot{m}_s W_2 \tag{3.5}$$

By similar procedure,

Heat Balance

$$Heat\ input = heat\ outlet + heat\ loss \tag{3.6}$$

thus

$$\dot{m}_a h_1 + \dot{m}_s H_1 = \dot{m}_a h_2 + \dot{m}_s H_2 + Q_L \tag{3.7}$$

where

Q_L=heat losses from the dryer outer cladding and structurel supports. For well-insulated

drying chambers heat losses are low.

3.4 Droplet/Particle Drying Mechanism

The theoretical modeling of the spray drying process is based on describing the drying behavior of individual droplets and particles. When droplets contain solids (either dissolved or suspended), the drying process is typically divided into two main stages. In the first drying stage, the droplet is exposed to a stream of hot drying gas (such as air, steam, or nitrogen). The droplet first absorbs sensible heat, and then evaporation begins. As moisture evaporates, the droplet shrinks and the concentration of solids near its surface increases. Eventually, solid material starts to deposit on the surface, forming a layer called a "crust." At this point, the droplet becomes a wet particle, and the second drying stage begins. In the second stage, the drying rate slows down due to the resistance created by the crust layer. The moisture inside the particle continues to evaporate until it reaches equilibrium with the surrounding drying gas. After this, drying effectively ends, and the particle is heated until it reaches the gas temperature. Typical changes in droplet temperature and moisture content during drying are illustrated in Figure 3.9:

The interval from point 0 to 1 shows initial heating,

Point 1 to 2 represents evaporation,

Point 2 to 3 corresponds to the second drying stage,

Point 3 to 4 marks the final heating to equilibrium.

The mathematical model describing single-droplet drying is then extended to represent the behavior of a spray containing millions of droplets. A realistic model must include the complex physical interactions in spray drying—among gas (drying medium), liquid (droplets), and solid (particles). Each of these phases is not a pure substance, but a mixture of several components. Therefore, both internal transport phenomena (within droplets or particles) and external transport phenomena (between gas and droplets/particles) must be considered for all phases in the drying chamber.

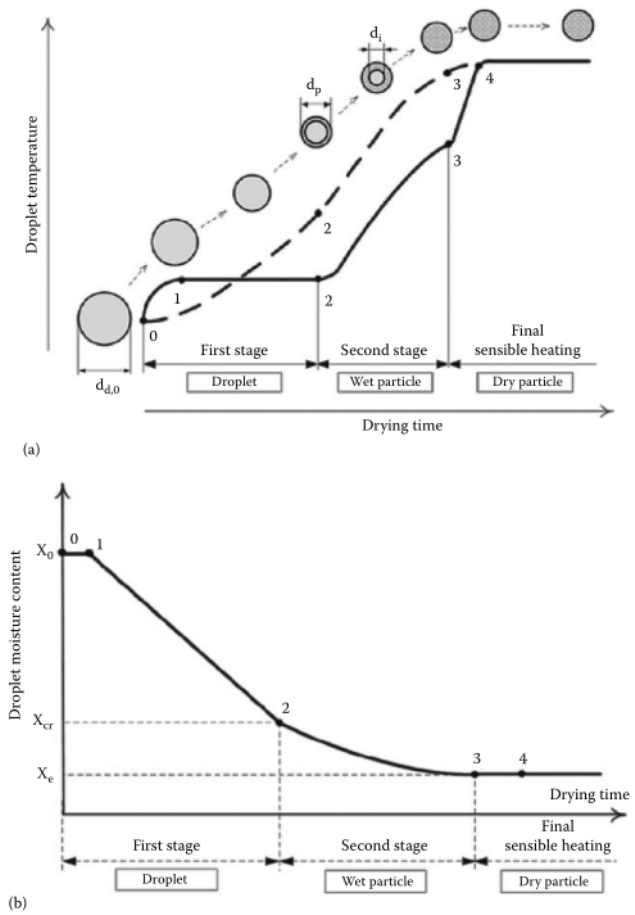

Figure 3.9. (a) droplet temperature, (b) droplet moisture content[2]

The theoretical modeling of such a system is complex. Therefore, some general simplifications are typically applied. A common and reasonable assumption is to treat the drying gas as a continuous phase, and the spray (droplets and particles) as a discrete phase. This is justified because, in spray dryers, the gas phase occupies a much larger volume than the dispersed droplets and particles.

The following assumptions are applicable to the single droplet/particle drying model used in this study:

1. There are no temperature/concentration gradients within the droplet/particle. Since the droplets are very small (200 μm), the variation of temperature within the droplet can be neglected.

2. Internal circulation inside the slurry droplet is neglected. The droplet sizes are relatively small and the presence of solid particles inside the droplet hampers internal circulation of the liquid.
3. The droplets and the resulting particles remain spherical throughout the tower.
4. The density and specific heat of the slurry, and the diffusivity of vapours into the bulk remain constant.
5. Only the first drying stage has been modeled.

When droplets move relative to the surrounding air, the airflow around them affects their evaporation rate. To calculate the mass and heat transfer rates, both the flow conditions around the droplet and its physical properties are considered. These effects are typically represented using combinations of dimensionless numbers.

Table 3.1. Dimensionless numbers

Group	**Significance**	**Symbol**
Reynolds (Re)	$\frac{inertia\ force}{viscous\ force}$	$\frac{\rho_a v_p D_p}{\mu_a}$
Prandlt (Pr)	$\frac{kinematic\ diffusivity}{thermal\ diffusivity}$	$\frac{c_{pa}\mu_a}{k}$
Schmidt (Sc)	$\frac{kinetic\ viscosity}{molecular\ diffusivity}$	$\frac{\mu_a}{D_{diff}\rho_a}$
Nusselt (Nu)	$\frac{total\ heat\ transfer}{conductive\ heat\ transfer}$	$\frac{h_c D_p}{k}$
Sherwood (Sh)	$\frac{mass\ diffusivity}{molecular\ diffusivity}$	$\frac{k_g D_p}{D_{diff}}$

3.4.1 Governing Equations

The motion of the droplets/particles is described by Newton's second law:

$$m_p \frac{dv_s}{dt} = \left(\rho_p - \rho_a\right)V_p g - 3f_D \mu \pi D_p v_s - v_s k_g A_p (P_W - P^0(T_a)) \tag{3.8}$$

The mass change equation of a particle:

$$\frac{dm_p}{dt} = k_g A_p (P_W - P^0(T_a)) \tag{3.9}$$

In the first stage of drying, the temperature within the evaporating spray droplet is assumed to be uniform across its radius. Based on this assumption, the energy conservation for the droplet is expressed by the following equation:

$$m_p c_{pL} \frac{dT_p}{dt} = h_c A_p \left(T_a - T_p\right) + k_g A_p (P_W - P^0(T_a))\lambda \tag{3.10}$$

The equation describing the axial position of the particle:

$$\frac{dz}{dt} = v_p \tag{3.11}$$

The correlations used for this study are as follows.

Nusselt number:

$$Nu = 2 + 0.4Re^{0.5}Pr^{0.33} \tag{3.12}$$

Sherwood number:

$$Sh = 2 + 0.4Re^{0.5}Sc^{0.33} \tag{3.13}$$

Drag coefficient:

$$C_D = 24/Re(1 + 0.14Re^{0.7}) \quad (3.14)$$

The thermophysical properties of air and milk used in the solution are given in Table 3.2

Table 3.2. Parameters

Parameter	**Value**
Q_{milk}	1900 kg/h
T_{a0}	403 K
T_{p0}	303K
P	101325 Pa
c_{pL}	4184 J/kgK
c_{pa}	1046 J/kgK
λ	2259360 J/kg
ρ_L	1000 kg/m^3
μ_a	$2.3x10^{-5}\ kg/ms$
k	$0.033472\ J/msK$
D_{diff}	$1.8x10^{-5}m^2/s$
ρ_{milk}	440 kg/m^3
W_{in}	20 kg/kg
ω_{in}	0 kg/kg
Q_{air}	20 kg/s
W_{out}	0.005 kg/kg

3.5 Discrete Phase Model (DPM)

The DPM is a multiphase flow model in which the continuous phase (air) is solved using the Eulerian approach, while the dispersed phase (droplets) is tracked using a Lagrangian framework. In this model, droplets are treated as discrete particles whose position, velocity, temperature, and mass are computed over time as they move through the flow field. The DPM allows for the simulation of momentum, heat, and mass transfer interactions between the droplet phase and the surrounding gas.

Key physical phenomena captured by the DPM in spray drying simulations include:

- Droplet motion: The trajectories of droplets are influenced by drag and gravity forces. The equations of motion are solved using Newton's second law.
- Heat transfer: Convective heat transfer occurs between the droplets and the hot air, raising the droplet temperature.
- Evaporation: Once the droplet surface reaches the saturation temperature, mass transfer takes place, leading to a reduction in droplet mass and addition of vapor to the air phase.
- Drying behavior: In advanced DPM formulations, the formation of a dry outer shell and internal moisture diffusion within the droplet can also be modeled.

The DPM is particularly suitable for dilute systems, where the dispersed phase occupies a relatively small volume fraction. Using this model, it is possible to predict key performance indicators such as temperature distribution, droplet evaporation time, moisture content profiles, and final powder characteristics within the spray drying chamber.

3.6 CFD Modelling

The numerical solution of external transport phenomena in both the continuous and discrete phases, as well as the computational simulations, were carried out using a 3D pressure-based solver within the computational fluid dynamics (CFD) software ANSYS FLUENT. This solver is built on the finite volume method and supports a two-way coupled Euler–Lagrange approach to model interactions between the continuous and discrete phases. The drying chamber geometry was meshed using 2.5M structured grid cells, which consisted of hex elements of varying sizes.

All numerical simulations of the spray drying process were carried out in steady-state, using a two-way coupling approach. For the continuous phase, spatial discretization of the conservation equationswas performed using a second-order upwind scheme. The SIMPLE (Semi-Implicit Method for Pressure-Linked Equations) algorithm was used to couple pressure and velocity fields.

For the dispersed phase, the particle tracking scheme was automatically selected based on solution stability, switching between low-order implicit and high-order trapezoidal methods as needed. The Discrete Phase Model (DPM) sources were updated at each iteration of the continuous phase solution. The entire steady-state formulation maintained second-order accuracy.

The simulation followed a specific strategy:

1. First, the airflow field (drying gas) was solved without droplets, until a converged solution was obtained.
2. Then, spray droplets were introduced into the domain, and two-way coupled calculations were performed until a new converged steady-state solution was reached.

Both dry air and droplets enter the chamber from the same surface and exit from the same surface. The upper section of the chamber is defined as the inlet boundary, while the lower section is defined as the outlet boundary (Figure 3.10).

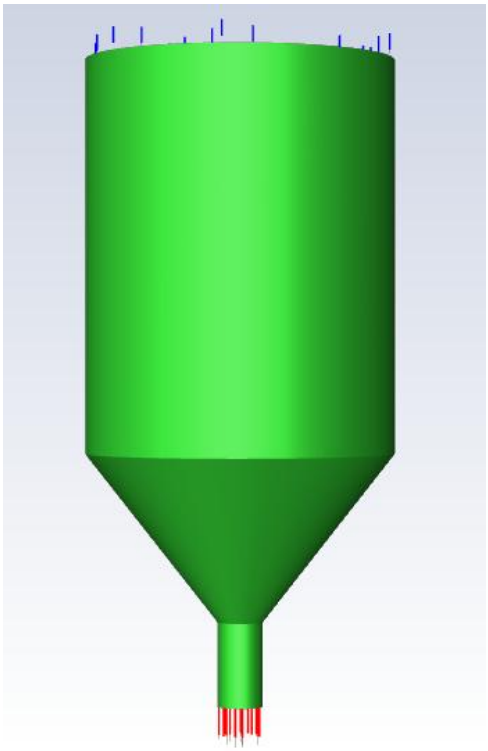

Figure 3.10. inlet, outlet boundary conditions

4. FINDINGS AND DISCUSSIONS

This section presents and discusses the analytical and numerical results obtained from both the MATLAB model and ANSYS Fluent simulations of the spray drying process.

4.1 Droplet Mass vs. Position

The plot of droplet mass along the vertical position in the drying chamber indicates a continuous reduction in mass due to evaporation. The steepest decline is observed in the initial section, confirming that the majority of moisture is removed in the early stages of drying. This aligns well with literature findings and supports the assumption that heat and mass transfer rates are highest at the top of the chamber, where the temperature and humidity gradients are strongest.

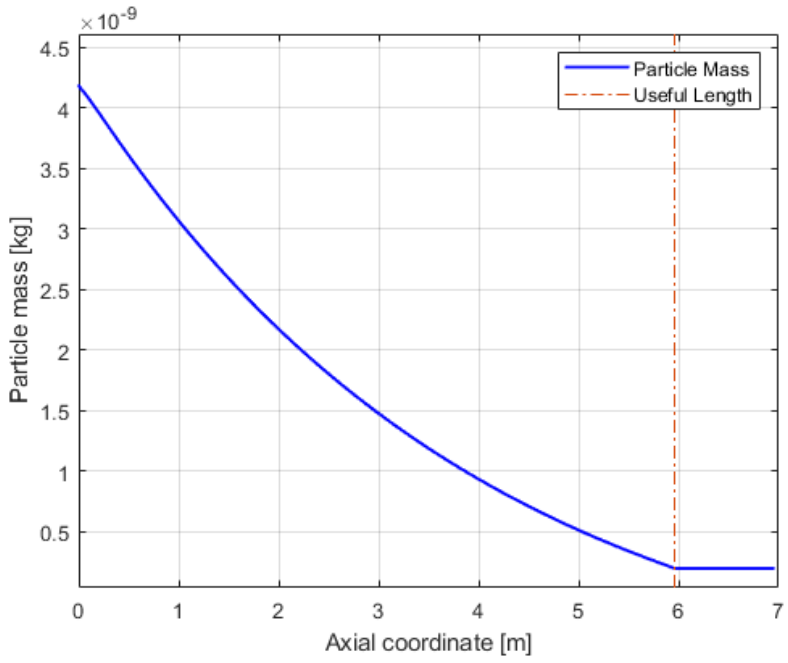

Figure 4.1. Particle mass-position plot

4.2 Droplet and Air Temperature vs. Position

The temperature-position graph reveals a sharp increase in droplet temperature during the initial seconds of drying, followed by a plateau, reflecting the constant-temperature drying period. In contrast, the air temperature gradually decreases along the flow direction as it transfers heat to the droplets. This inverse relationship is consistent with energy conservation principles and validates the co-current drying model used.

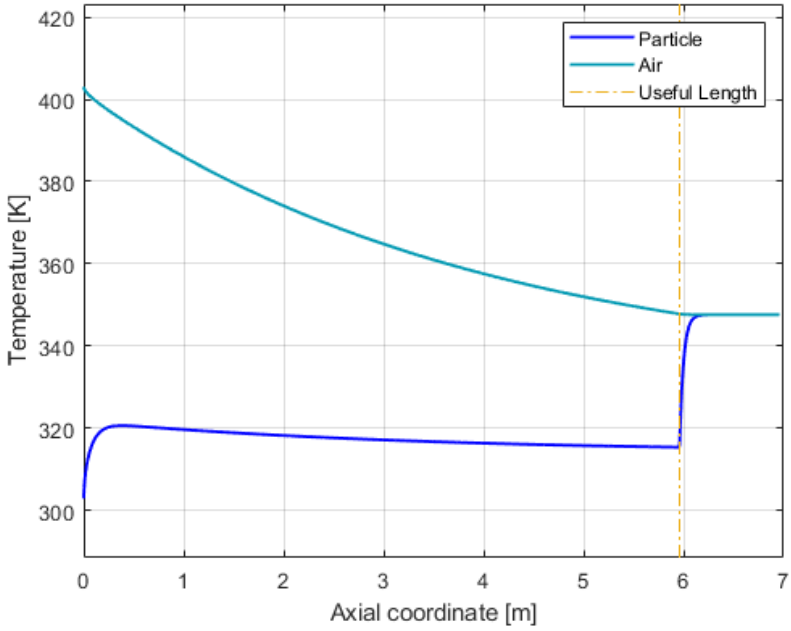

Figure 4.2. Temperature-position plot

4.3 Droplet Velocity vs. Position

The velocity-position profile shows that the droplet accelerates immediately after injection due to gravitational and drag forces but stabilizes after a short time. The terminal velocity is reached once the drag force balances gravity. This behavior indicates that droplet dynamics can be accurately predicted using force balance equations within the Lagrangian framework.

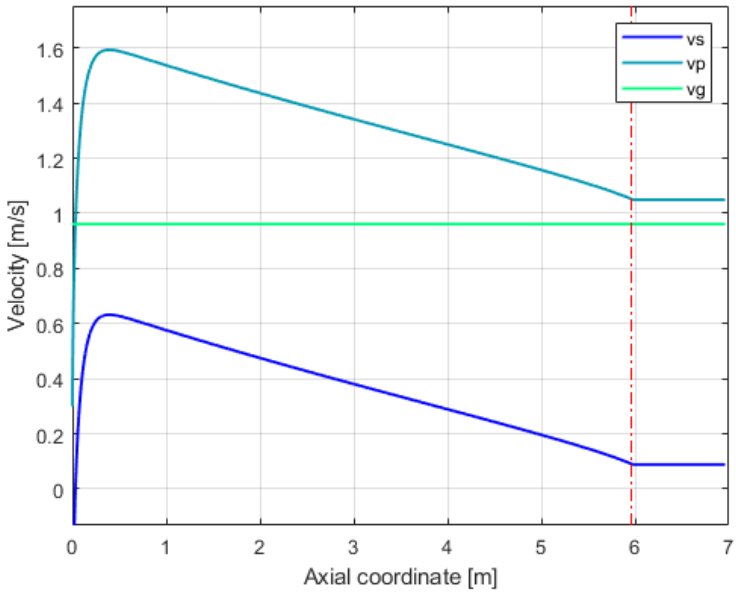

Figure 4.3 Velocity-position plot

4.4 Moisture Content of Droplet vs. Position

This graph shows a significant drop in moisture content within the first half of the drying chamber, mirroring the mass loss trend. As the drying progresses, the rate of moisture removal decreases due to reduced vapor pressure gradients. This confirms the transition from constant-rate drying to falling-rate drying phases.

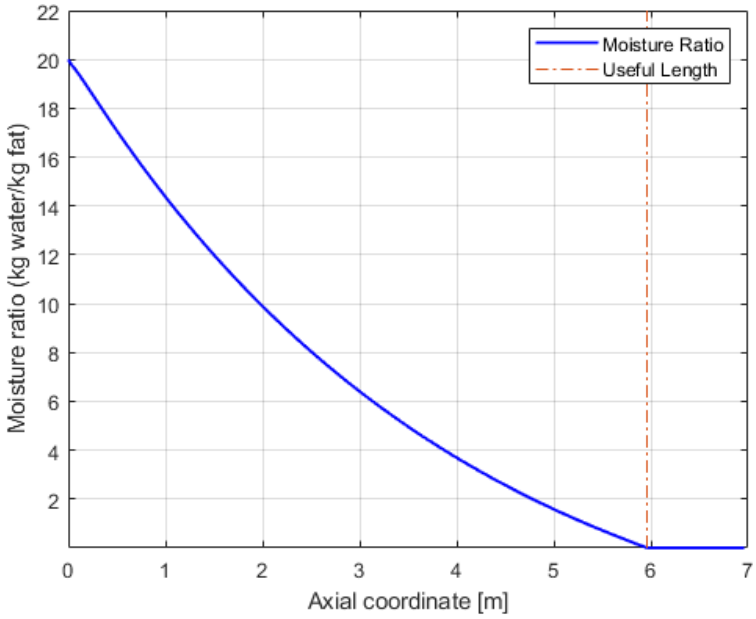

Figure 4.4 Moisture content-position plot

4.5 Absolute Humidity of Air vs. Position

As expected, the absolute humidity of the air increases along the vertical axis due to moisture uptake from evaporating droplets. The change in slope of the curve suggests variable evaporation rates at different heights and is consistent with the observed decline in droplet moisture content.

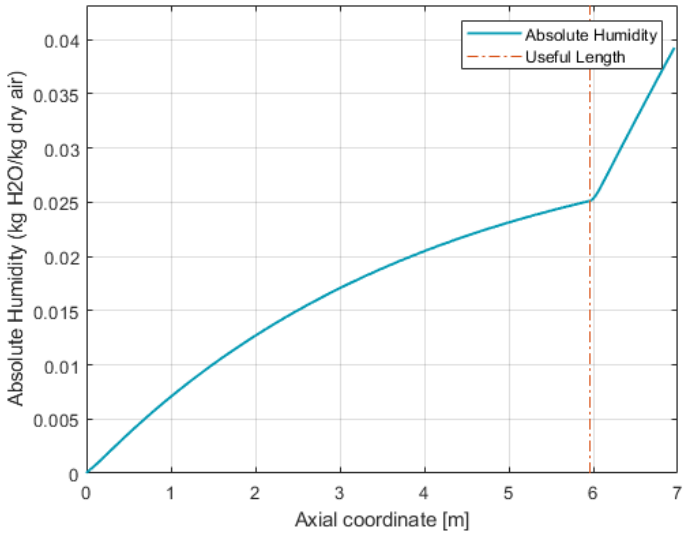

Figure 4.5. Absolute humidity-position plot

4.6 Temperature Contour (ANSYS Fluent)

The temperature contour obtained from ANSYS Fluent displays the spatial distribution of air temperature inside the spray dryer chamber. The highest temperature region is located near the air inlet at the top of the chamber, where the hot drying air first contacts the droplets. As the air flows downward in co-current fashion with the droplets, it gradually loses heat due to energy transfer to the droplets. The contour illustrates a smooth temperature gradient from top to bottom, confirming that the majority of the heat transfer occurs in the upper half of the chamber. Localized cooling zones may also be observed where droplet density is higher, leading to more intense heat exchange. This visualization supports the results obtained from the MATLAB temperature-position plot and helps identify thermal zones where drying is most efficient.

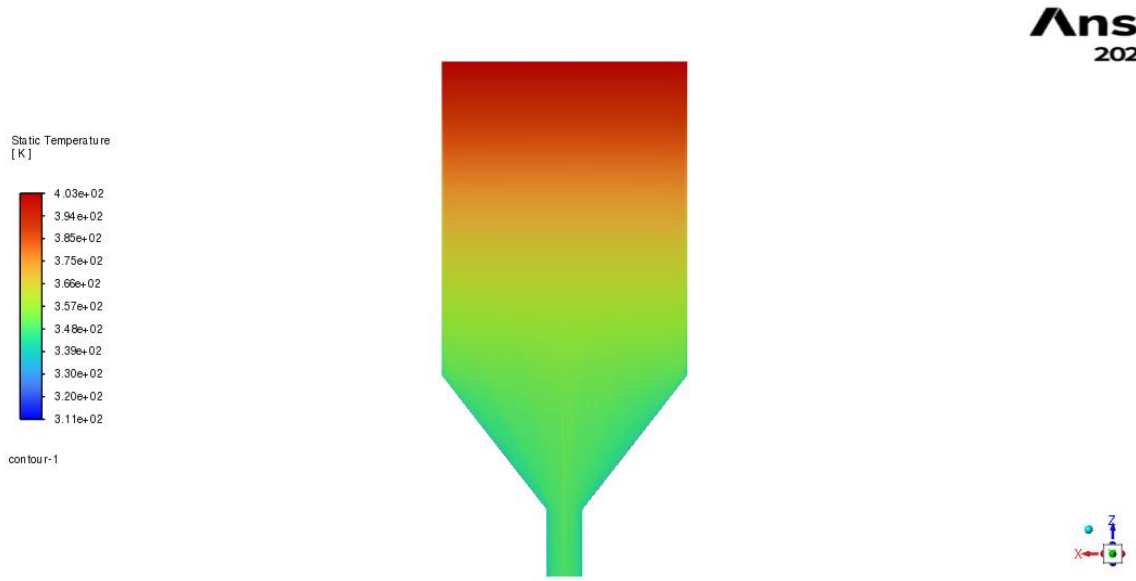

Figure 4.6 Temperature contour

4.7 Mass Fraction of H_2O Contour (ANSYS Fluent)

The contour of water vapor mass fraction provides insights into the spatial distribution of moisture content in the air during the drying process. As droplets evaporate, the surrounding air becomes increasingly saturated with water vapor. The contour clearly shows rising mass fraction values in the regions where droplets are concentrated, particularly in the upper and middle sections of the chamber. This increase is consistent with the absolute humidity-position results obtained from the MATLAB model.

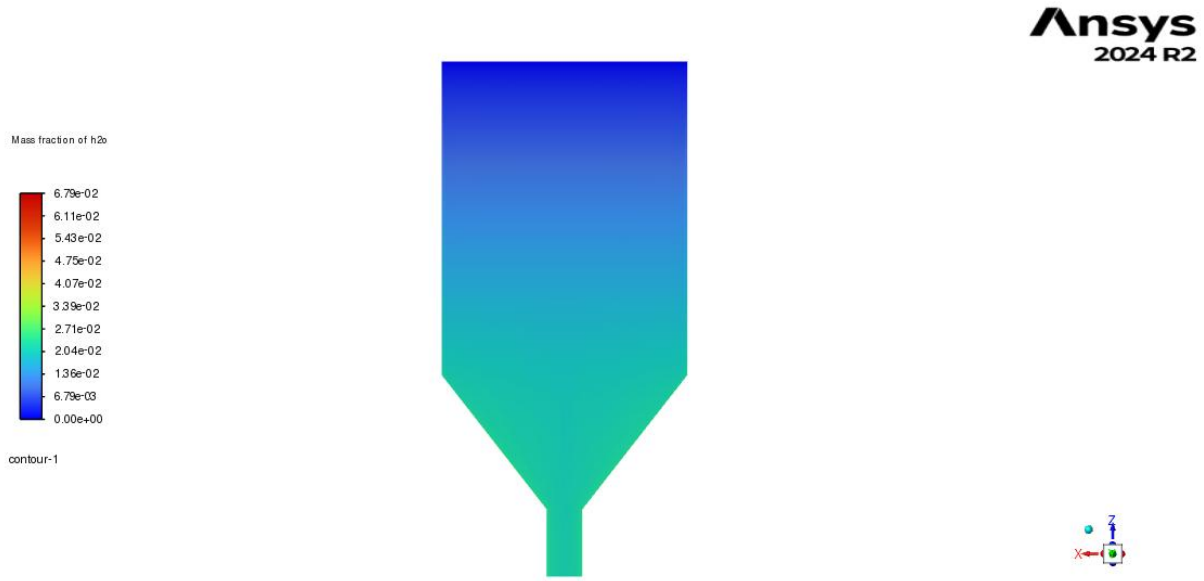

Figure 4.7. Mass fraction of H_2O contour

4.8 Particle Pathlines (ANSYS Fluent)

The particle pathline plot visualizes the trajectories of droplets as they travel through the spray dryer chamber under the influence of gravity, drag, and buoyant forces. The paths confirm that droplets follow a co-current downward motion with the drying air, consistent with the assumed operating conditions. The simulation shows that most droplets follow a smooth, vertical path from the injection point to the outlet.

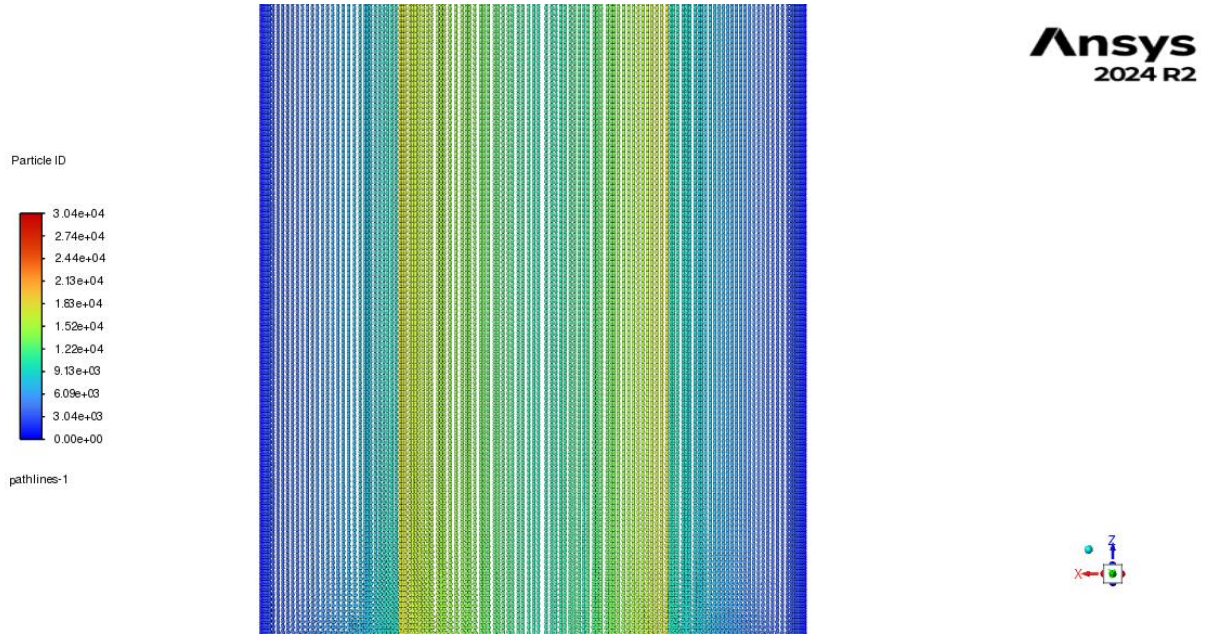

Figure 4.8 Pathline of particles

Overall, the results from both the theoretical and numerical models show strong agreement in predicting key trends such as moisture loss, temperature evolution, and droplet dynamics. While the MATLAB model provides a fast and reliable method for evaluating process behavior along the chamber axis, the ANSYS Fluent simulations give a more detailed understanding of spatial variations and flow behavior. The integration of both approaches ensures robust process analysis and lays a foundation for future experimental validation and scale-up.

5. RESULTS

The project focused on modeling and simulating the spray drying process to better understand the heat and mass transfer mechanisms involved. Key outcomes of the study are summarized below:

- A one-dimensional theoretical model was developed in MATLAB to predict droplet temperature, moisture content, and diameter changes along the drying chamber.
- The model showed that most of the drying occurs in the upper half of the chamber where temperature gradients are highest.
- A CFD model was created in ANSYS Fluent using the Discrete Phase Model (DPM), which accurately simulated droplet trajectories and evaporation behavior.
- CFD results supported the theoretical model's predictions and provided additional insight into air flow behavior and droplet-air interactions.

Additional Considerations:

- The combination of theoretical and CFD modeling was effective for both preliminary analysis and detailed process evaluation.
- No safety hazards exist for the current simulation-based work; however, real spray drying systems must consider high temperature and pressure risks.
- The study complies with legal and ethical standards. All software tools were used under institutional licenses, and existing models were properly cited.

Conclusion:

The study demonstrates that combining simplified analytical models with detailed CFD simulations offers a robust and efficient method for analyzing and optimizing spray drying processes. The results provide a useful basis for future experimental validation and scale-up applications.

REFERENCES

[1] Masters, K. (1972). Spray Drying: An introduction to Principles, Operational Practice and Applications. London: Leonard Hill Books.

[2] Mujumdar, A.S. (1987). Handbook of Industrial Drying. New York: Marcel Dekker

[3] Çengel, Y. A., & Boles, M. A. (2015). *Thermodynamics: An engineering approach* (8th ed.). New York, NY: McGraw-Hill Education.

[4] Çengel, Y. A., & Ghajar, A. J. (2015). Heat and mass transfer: Fundamentals and applications (5th ed.). New York, NY: McGraw-Hill Education.

[5] Keey, R. B., 1978. Introduction to industrial drying operations. Pergamon Press, Oxford.

[6] Crank, J. (1975). The Mathematics of Diffusion. Oxford: Clarendon Press, second edn.

[7] Arnanson, G. and Crowe, C. T. (1980). Assessment of numerical models for spray drying. Drying 1980 – Proceedings of the 2nd international drying symposium (IDS 1980), vol. 2, pp. 410-416.

[8] Bakker, A. 2002. Computational Fluid Mixing. NH, USA: Fluent Inc.

[9] Chen, X. D. and Lin, S. X. Q. (2005). Air drying of milk droplet under constant and time dependent conditions. AICHE J., vol. 51, No. 6, pp. 1790-1799.

[10] Crowe, C. T. (1980). Modeling spray-air contact in spray-drying systems. Advances in drying, vol. 1, pp. 63-99.

[11] Crowe, C. T. (1983). Droplet-gas interaction in counter-current spray dryers. Drying Technology, vol. 1, pp. 35-56.

[12] Dalmaz, N., Ozbelge, H. O., Eraslan, A. N. and Uludag, Y. (2007). Heat and Mass Transfer Mechanisms in Drying of a Suspension Droplet: A New Computational Model. Drying Technology, vol. 25 (2), pp. 391-400.

[13] Ali, M., Mahmud, T., Heggs, P. J., Ghadiri, M., Djurdjevic, D., Ahmadian, H., Juan, L. M., Amador, C. and Bayly, A. (2014). A one-dimensional plug-flow model of a counter-current spray drying tower. Chem. Eng. Res. Des., vol. (92), pp. 826-841.

[14] Parti, M. and Palancz, B. (1974). Mathematical model for spray drying. Chem. Eng. Sci., vol. 29, pp. 355-362.

[15] Patel, K. C. and Chen, X. D. (2005). Prediction of spray-dried product quality using two simple drying kinetics models. J. Food Process Eng., vol. 28, pp. 567-594.

[16] Perry, R.H. and Green, D.W. (1997). Perry's Chemical Engineer's Handbook. New York, McGraw-Hill, Seventh Edn.

[17] https://commons.wikimedia.org/wiki/File:Psychrometric_chart_%28altitude_0,_750,_1500,_2250,_3000_m%29.pdf

[18] https://gyansanchay.csjmu.ac.in/wp-content/uploads/2022/01/Drying-I.pdf

[19] https://www.icapsulepack.com/spray-dryer/

[20] https://spraytechsystem.com/three-most-important-components-in-the-spray-dryer.html

[21] Saleh, S. N. (2010). CFD simulations of a co-current spray dryer. WASET, vol. 62, pp. 772-777.

[22] Sharma, S. (1990). Spray dryer simulation and air flow pattern studies, Ph.D. Thesis, The University of Aston, Birmingham, UK.